Research Square

Preprints are preliminary reports that have not undergone peer review.
They should not be considered conclusive, used to inform clinical practice,
or referenced by the media as validated information.

Constructing highly robust biocomposite films via one-pot multi- point crosslinking mediated by dialdehyde carboxymethyl cellulose for sustainable and active packaging

Wei Ding

dingwei1368@bipt.edu.cn

Beijing Institute of Petrochemical Technology

Xuehai Gong

Beijing Institute of Petrochemical Technology

Xinyue Wang

Beijing Institute of Petrochemical Technology

Yanbei Wu

Beijing Technology and Business University

Rong Wang

Beijing University of Chemical Technology

Xi Qi

Beijing University of Chemical Technology

Zhengyu Zhao

Beijing Institute of Petrochemical Technology

Kanglei Wang

Technical Institute of Physics and Chemistry

Research Article

Keywords: Dialdehyde carboxymethyl cellulose, Catechin, Rare-earth salts, Bioactivity, Mechanical strength

Posted Date: May 19th, 2026

DOI: https://doi.org/10.21203/rs.3.rs-9721849/v1

License: This work is licensed under a Creative Commons Attribution 4.0 International License.
Read Full License

Additional Declarations: No competing interests reported.

Constructing highly robust biocomposite films *via* one-pot multi-point crosslinking mediated by dialdehyde carboxymethyl cellulose for sustainable and active packaging

Wei Ding [a,*], Xuehai Gong [a], Xinyue Wang [a], Yanbei Wu [e,*], Rong Wang [d], Xi Qi [d], Zhengyu Zhao [a], Kanglei Wang [b,c,*]

[a] College of New Materials and Chemical Engineering, Beijing Institute of Petrochemical Technology, Beijing 102617, P. R. China

[b] Technical Institute of Physics and Chemistry, Chinese Academy of Sciences, Beijing 100190, P. R. China

[c] China Leather and Footwear Research Institute Co., Ltd., Beijing 100015, P. R. China

[d] State Key Laboratory of Chemical Resource Engineering, Beijing University of Chemical Technology, Beijing, 100029, P. R. China

[e] China-Canada Joint Lab of Food Nutrition and Health (Beijing), School of Food and Health, Beijing Technology and Business University, Beijing, 100048, P. R. China

Corresponding authors:

Wei Ding: dingwei1368@bipt.edu.cn

Yanbei Wu: yanbeiwu@btbu.edu.cn

Kanglei Wang: wkljy1226@163.com

Abstract

Developing biodegradable packaging materials is essential for advancing environmental sustainability and social well-being. Herein, dialdehyde carboxymethyl cellulose (DCMC) was synthesized through the selective oxidation of carboxymethyl cellulose using sodium periodate. Then, gelatin/DCMC/catechin/rare-earth-ion composite films (GDCR) with varying DCMC contents were fabricated via a one-pot process using DCMC, catechin, rare-earth ions, and gelatin. SEM, FTIR, and XRD confirmed favorable compatibility and strong interactions among DCMC, catechin/rare-earth ions, and gelatin. The GDCR film with 10% DCMC content ($GD_{10\%}CR$) displayed better mechanical strength, and its tensile strength (46.37 MPa) was increased by 107.10% compared to that of the pure gelatin film. Besides, enhanced thermal stability, excellent UV, moisture, and gas barrier properties, enhanced resistance to swelling and dissolution, and favorable antioxidant properties were also demonstrated. Notably, due to multipoint crosslinking among DCMC, gelatin, and catechin/rare-earth ions, the GD10%CR films exhibited significant antibacterial activity, with inhibition ratios of 91.85% against *S. aureus* and 90.00% against *E. coli*. Moreover, a real-time study of GDCR as a fruit packaging material was conducted on blueberries, showing that GDCR could maintain their freshness for up to 4 days at room temperature. Overall, the as-prepared GDCR films show great promise for applications in sustainable food packaging.

Keywords: Dialdehyde carboxymethyl cellulose; Catechin; Rare-earth salts; Bioactivity; Mechanical strength

1. Introduction

Packaging plays a crucial role in maintaining the safety, quality, and nutritional integrity of food and specialized products throughout their entire lifecycle. In recent years, the environmental problems stemming from the non-biodegradable nature of petroleum-based plastics have intensified, posing a significant global challenge that requires immediate attention (Kamau-Devers and Miller 2020). A substantial amount of petroleum-based plastic products is either sent to landfills or released into the natural environment, resulting in "white pollution" that poses serious threats to soil and marine ecosystems. Although this problem is widely recognized, petroleum-based plastics remain the predominant materials used in food packaging due to their affordability, ease of processing, and superior barrier characteristics (Tyuftin and Kerry 2021). Nonetheless, the adverse effects of commonly used plasticizers, including phthalates and bisphenol A, on food quality and human health must not be overlooked (Robinson and Miller 2015; Carmen 2021; Kumari et al. 2023). Consequently, the food packaging industry is undergoing a green revolution to address these challenges and improve the environmental and safety aspects of food packaging (Wu et al. 2023).

With ongoing in-depth research on natural biopolymers, green packaging based on them and their combinations has become one of the most promising alternatives for addressing the current problems (Singh and Devi 2019; Z. Naser et al. 2021; Mori 2023; Yin and Wai Woo 2024). Gelatin is a water-soluble protein obtained by hydrolyzing animal collagen. Due to its low biotoxicity, low cost, special film-forming ability, and biodegradability, it has been widely studied and applied in the development of food packaging films (Karim and Bhat 2008; Lu et al. 2022; Luo et al. 2022; Beghetto et al. 2026). However, the practical application of pure gelatin films is limited by their inherent mechanical weaknesses, high solubility, poor

barrier properties, and inadequate antibacterial and antioxidant capabilities (Fraga and Williams 1985; Białopiotrowicz and Jańczuk 2002; Santandrea and Beghetto 2025). To overcome these limitations, combining gelatin with other biopolymers through interactions such as hydrogen bonding has proven effective. For example, biopolymers such as chitosan, starch, soy protein isolate, and carboxymethyl cellulose (CMC) have been incorporated into gelatin films to meet their needs in the field of use (Cao et al. 2007; Al-Hassan and Norziah 2012; Fakhouri et al. 2013; Nazmi et al. 2017; Qiao et al. 2017; Ding et al. 2025). CMC is a substance derived from cellulose, in which the hydroxyl groups on the cellulose chains are substituted by carboxyl groups. Due to its low cost, stable chemical properties, good solubility, and rich functional group structure, it has significant economic feasibility in the food industry (Kong et al. 2024). In recent years, sodium periodate has been used to selectively oxidize CMC to prepare dialdehyde carboxymethyl cellulose (DCMC) (Jiang et al. 2016). This biomass-derived compound has been used as a reinforcing agent for biopolymer materials because it is mild, biocompatible, and easy to form films (Kurhade et al. 2024). The aldehyde groups of DCMC are able to react with the amino groups of gelatin through the Schiff base reaction, significantly enhancing the crosslinking degree and strength of gelatin-based films (Wang et al. 2019; Yu et al. 2022; Ding et al. 2024).

Food packaging plays a crucial role in reducing microbial transmission and preventing cross-contamination, underscoring the urgent need for safe and effective novel antibacterial food packaging materials (Threlfall et al. 2000; Caniça et al. 2019; Omerović et al. 2021). Catechin, a flavanol found in plants such as tea, exhibits high chemical reactivity due to the ortho-hydroxyl groups in its molecular structure. This reactivity enables catechin to form stable five-membered chelate rings with metal ions (Mira et al. 2002; Leopoldini et al. 2011). Furthermore, catechin can form complexes with polysaccharides, lipids,

alkaloids, and DNA, thereby exerting inhibitory effects against a broad spectrum of microorganisms (Mendoza-Wilson and Glossman-Mitnik 2006; Liu et al. 2016; Lee et al. 2020). Owing to their unique electronic structures, rare earth ions can readily coordinate with the ortho-hydroxyl groups of catechin to generate stable complexes. This coordination not only mitigates the high water solubility of rare-earth ions but also reduces catechin instability (Liu et al. 2020a). More importantly, such interactions significantly enhance the membrane permeability and antibacterial activity of catechin. Notably, catechin serves as an effective carrier to facilitate the entry of rare earth metals into microbial cells. Meanwhile, catechin can interact with proteins, peptides, and glycoproteins, further enhancing antibacterial activity. As a result, the catechin–rare earth metal complexes exhibit a distinct synergistic antibacterial effect, highlighting the crucial role of rare earth metals in strengthening the system's overall antibacterial activity (Liu et al. 2020b). Given these features, it can be hypothesized that fully leveraging the synergistic effects of DCMC, catechin, and rare earth ions will yield highly robust and bioactive gelatin-based composite films for food packaging.

Hence, to address the existing challenges in gelatin-based food packaging materials, a novel strategy was proposed in this work to fabricate a gelatin-based food packaging film (GDCR). This film was designed to incorporate carboxymethyl cellulose sodium (DCMC) as a reinforcing agent and catechin/rare-earth ions as active antibacterial components, aiming to synergistically improve the mechanical and functional performance of gelatin-based packaging materials. To fully clarify the structure-function relationship of GDCR films, the structural characteristics of GDCR films with varying DCMC contents were systematically investigated, and the interactions among gelatin, DCMC, catechin, and rare-earth ions were comprehensively analyzed. On this basis, the functional properties (including mechanical and antibacterial properties) of the GDCR films were further explored, thereby laying a theoretical and

experimental foundation for the development of high-performance gelatin-based active food packaging materials.

2. Materials and methods

2.1. Materials

Carboxymethyl cellulose (CMC, molecular weight: 250,000 Da, degree of substitution: 0.7) and Lanthanum (III) nitrate hexahydrate ($La(NO_3)_3 \cdot 6H_2O$) were obtained from Sinopharm Chemical Reagent Co., Ltd. Gelatin, sodium periodate ($NaIO_4$), ethylene glycol and glycerin were purchased from Beijing Chemical Works Co., Ltd. Catechins, sodium hydroxide (NaOH), PBS buffer solution, potassium persulfate, hydrochloric acid and hydroxylamine hydrochloride were obtained from Shanghai Maclin Biochemical Technology Co., Ltd. Beef infusion powder, peptone, and agar powder were purchased from Qingdao Haibo Biotechnology Co., Ltd.

2.2. Preparation of DCMC

Dissolve 10.0 g of CMC in 200 mL of deionized water and stir continuously in the beaker at 50°C. When the solution temperature drops to 35°C, add 100 mL of $NaIO_4$ solution (0.11 g/mL) to the beaker containing the CMC solution. Adjust the pH to 3 with sulfuric acid solution (1 M) and react in the dark for 4 hours. Subsequently, an equivalent amount of ethylene glycol was added, and the resulting mixture was continuously stirred for 1 h to remove any unreacted $NaIO_4$. Excess anhydrous ethanol was then added to precipitate a white flocculent product, which was centrifuged to obtain at 8000 rpm for 5 min. The prepared precipitate was placed in a dialysis membrane with a molecular weight cut-off of 8,000~10,000 Da to

remove impurities from the system. Finally, the resulting DCMC was freeze-dried and stored in a sealed desiccator for subsequent use.

2.3. Determination of aldehyde content of DCMC

To quantitatively determine the aldehyde group content, accurately weigh 0.5 g of the DCMC sample. Dissolve this sample in 25 mL of distilled water, then transfer the solution to a beaker for thorough stirring. Hydroxylamine hydrochloride (20 mL, 0.72 mol/L) was added, and the pH was adjusted to 5 using 0.1 M NaOH solution. The reaction was carried out at 40°C and lasted 4 h. Afterward, the pH was readjusted to 5 by adding NaOH solution (1 mol/L), and the final volume was denoted as V_c (L). For the control experiment, an equal amount of CMC was used under identical conditions, and the volume of NaOH solution was denoted as V_b (L). The aldehyde content of DCMC was then determined using **Eq. 1**.

$$W_{AC}\ \%=\frac{M_{NaOH}(V_c\text{-}V_b)}{m/211}\times 100 \quad \textbf{(1)}$$

2.4. Preparation of gelatin/DCMC/catechin/rare earth ions composite film

To prepare the gelatin-based composite films, 2 g of gelatin, 0.75 g of glycerol, and DCMC with different concentrations (10 wt%, 5 wt%, and 2.5 wt% of gelatin) were added to 50 mL of distilled water in a flask at 60°C. The mixture was stirred until completely dissolved, and the pH was adjusted to 7~8. The temperature of the reaction was maintained under 60°C for 4 h and then was turned to 40°C. Next, 0.1 g of catechin was added, and the pH was turned to 4~4.5, allowing the reaction to continue for 2 h. Subsequently, 0.0236 g of $La(NO_3)_3 \cdot 6H_2O$ was added, and the reaction continued for an additional 2 h. To remove bubbles, the mixture was subjected to ultrasonic treatment for 20 min. The resulting solution was

then cast into a 20 × 20 cm mold plate, and after solvent evaporation, the Gelatin/DCMC/Catechin/Rare earth ions composite films (GDCRs) were prepared by peeling. Depending on the concentration of DCMC (2.5 wt%, 5 wt%, and 10 wt%), the as-prepared GDCRs were labeled as $GD_{2.5\%}CR$, $GD_{5\%}CR$, and $GD_{10\%}CR$, respectively. For comparison, pure gelatin films, gelatin-based films without catechin and rare earth ions, as well as gelatin-based film without DCMC were also prepared using the same method and labeled as GF, $GD_{10\%}$, and GCR, respectively.

2.5. Characterization

2.5.1. Fourier transform infrared spectroscopy (FTIR)

The FTIR spectra of powdery raw materials and composite films were measured by an FTIR spectrophotometer (TENSOR 27, Bruker, Germany) *via* KBr pressed disk (for powdery samples) or attenuated total reflectance (ATR) technique (for the composite films).

2.5.2. X-ray diffraction (XRD)

XRD patterns of the as-prepared composite films were recorded using an X-ray diffractometer (Ultima IV, Rigaku, Japan) equipped with a Cu Kα radiation source (k=0.154 nm) operating at 40 kV and 40 mA. The scanning speed was set to 8 °/min, covering a 2θ range of 5° to 60°.

2.5.3 Morphology observation

The surface morphology of the composite films was examined by SEM (S-7800, Hitachi, Japan) at an accelerated voltage of 10 kV. Before the test, the film sample was firmly fixed to the sample platform, and

then a thin layer of gold was deposited onto it under vacuum.

2.5.4. Thermal stability analysis

Simultaneous thermogravimetric analysis (TGA) was performed using an SDT Q600 thermal analyzer (PerkinElmer, USA). This analysis was carried out in a nitrogen atmosphere throughout the process. The heating rate was set to 20 °C/min, and the temperature interval ranged from 25°C to 800°C.

2.5.5. Water contact angle (WCA) test

WCA values of the composite films were determined using an optical contact angle goniometer (CAM 100, KSV Instruments Ltd., Finland). This compact video-based instrument can measure contact angles from 1° to 180° with a measurement accuracy of ±1°.

2.5.6. Gas permeability test

Firstly, the thickness of all composite films was measured by a micrometer (Mitutoyo 103-129, Japan). Ten random measurements were taken from different locations around each film and recorded to the nearest 0.001 mm. The average measurement was used as the film sample thickness. The water vapor transmission rate (WVP) of the composite film was detected by gravimetric analysis. In brief, a glass jar containing distilled water (20 g) was used to create a humidity source, maintaining a relative humidity of 75%. The jar was then covered with a composite film sample, and changes in the jar's weight were monitored at 0, 8, 16, 24, 32, 40, and 48 h at 25°C in a desiccator containing 98% concentrated sulfuric acid (0% relative humidity). The WVP was determined based on **Eq. 2**.

$$WVP=\frac{\Delta m\times d}{A\times t\times \Delta p} \quad \textbf{(2)}$$

where WVP is water vapor permeability ($g\cdot m^{-1}\cdot s^{-1}\cdot Pa^{-1}$), Δm represents the change in weight of the jar (g), d represents the thickness of the GDCRs (m), A represents the exposed area of the GDCRs (m^2), t represents the time (s), and Δp represents the difference in partial pressure across the film sample (Pa).

Oxygen permeability coefficient (OPC) and carbon dioxide permeability coefficient (CPC) of the composite films were measured separately at 23°C and a relative humidity of 30 ± 1%, utilizing a Pressure Differential Gas-Tran Determinator N500 2.0 (Guangzhou Biaoji Packaging Equipment Co., Ltd., Guangzhou, China) in accordance with ISO 2556. Each film specimen was mounted on a stainless steel mask with an exposed testing area of 50 cm^2. A continuous nitrogen gas flow was applied to one side of the film, while either oxygen (O_2) or carbon dioxide (CO_2) gas was delivered to the opposite side under the same controlled conditions. The gas permeability coefficient (GPC) was calculated using **Eq. 3**.

$$GPC=\frac{V\times d}{A\times t\times \Delta p} \quad \textbf{(3)}$$

where *GPC* represents OPC or CPC ($cm^3\cdot\mu m\cdot m^{-2}\cdot d^{-1}\cdot kPa^{-1}$), V represents the volume of O_2 or CO_2 passed through the composite film (cm^3), d represents the thickness of the composite film (μm), A represents the exposed area of the composite film (m^2), t represents the time (day), Δp represents O_2 or CO_2 partial pressure difference (kPa).

2.5.7. Swelling behavior (SB) and water solubility (WS) analyses

In accordance with GB/T 1040.3-2006, 3 pieces of 1 cm × 2 cm test slices were cut off from each film sample. These were first dried at 40 °C for 12 h and weighed to record the initial mass as m_0. The slices were then immersed in distilled water and permitted to soak at ambient temperature for 24 h until fully

swollen. After soaking, the surfaces of the swollen samples were wiped dry with filter paper, and the final swollen mass was recorded as m_1. The samples were then dried at 40 ℃ for an additional 12 h, and the mass was re-recorded as m_2. All experiments were conducted in parallel and repeated three times. The final results are presented as the average of the data obtained from these three repetitions. The SB of the films was calculated using **Eq. 4**.

$$W_{sb}\ \%=\frac{m_1-m_0}{m_0}\times 100 \quad \textbf{(4)}$$

The WS of the films was computationally derived in accordance with **Eq. 5**.

$$W_{ws}\ \%=\frac{m_0-m_2}{m_0}\times 100 \quad \textbf{(5)}$$

2.5.8. Optical property analysis

The color parameters (including L^*, a^*, and b^* values) of the films were measured by a colorimeter (NH300, 3nh Technology Co., Ltd., China). Before the L^*, a^*, and b^* values of composite film samples were measured at five random positions on each film, a white standard plate ($L = 96.74$, $a = 0.36$, $b = 0.61$) should be chosen to calibrate the colorimeter. The total color difference (ΔE) was calculated using **Eq. 6**.

$$\Delta E=\sqrt{\left(L-L^*\right)^2+(a-a^*)^2+\left(b-b^*\right)^2} \quad \textbf{(6)}$$

2.5.9. Tensile strength measurement

The tensile stress-strain curve of the film sample was measured and analyzed by using a universal tensile testing machine (Instron 5966, Instron Corporation, USA). The sample was fabricated into standard dumbbell-shaped specimens measuring 50 mm × 4 mm × 0.5 mm, with a tensile testing rate established at 20 mm/min. The tensile strength was calculated according to **Eq. 7**.

$$T=\frac{F}{S} \quad \textbf{(7)}$$

where T is tensile strength (Pa), F is breaking strength (N), S is the cross-section area of film (m^2).

2.5.10. Antioxidant property evaluation

According to the DPPH and $ABTS^+$ radical scavenging methods previously reported (Luo et al. 2021), the antioxidative potential of the membrane samples was assayed using a ultraviolet-visible spectrophotometer. 0.1 g of the composite film samples was placed into a tube containing 5.0 mL of a 70% (v/v) methanol solution to extract the active compounds. After incubation at 25°C for 24 h, the supernatant was collected to determine the free radical-scavenging activities against DPPH and $ABTS^+$.

To measure the DPPH radical scavenging activity, 4 mg of DPPH was dissolved in 100 mL of methanol to prepare a DPPH methanol solution. After that, 4.0 mL of this solution and 2.0 mL of film sample extraction solution were fully mixed, left in the dark for 30 min, and then the absorbance at 517 nm was measured. As a control, DPPH solution was prepared without the addition of film sample extraction solution, which was replaced by methanol solution. The DPPH radical scavenging ratio (%) was calculated according to **Eq. 8**.

$$\text{DPPH radical scavenging ratio } \% = \frac{A_c - A_s}{A_c} \times 100 \quad \textbf{(8)}$$

where A_c and A_s stand for the absorbance of the DPPH solution from the control group and the composite membrane sample, respectively, measured at a wavelength of 517 nm.

The $ABTS^+$ radical scavenging ratio (%) was calculated according to **Eq. 9**.

$$ABTS^+ \text{ radical scavenging ratio } \% = \frac{A_0 - A_T}{A_0} \times 100 \quad \textbf{(9)}$$

where A_0 and A_T denote the absorbance of the $ABTS^+$ solution from the control group and the composite membrane sample, respectively, measured at 734 nm.

2.5.11. Antibacterial properties assessment

To evaluate the antibacterial properties of the composite films, as previously reported (Sun et al. 2024), *E. coli* (ATCC 25922) and *S. aureus* (ATCC 25923) were chosen as model bacteria for the present study, using the electroplating counting method. Calculate the growth suppression rate of the film sample against bacteria using **Eq. 10**.

$$\text{Growth inhibition ratio } \% = \frac{N_0 - N_1}{N_0} \times 100 \quad \textbf{(10)}$$

where N_0 and N_1 respectively represent the count of visible colonies in the control group and the membrane sample group.

2.5.12. Packaging application for blueberries

The blueberry samples (each weighing approximately 10 g, purchased from the local market) were placed in sealed plastic film packaging bags and stored in a constant temperature environment of (25 ± 2)℃ with a relative humidity of 60%~70% for 4 days. Take photos of the samples every 48 h to dynamically observe the deterioration of blueberries during storage. The preservation performance of the prepared composite film was evaluated by observing changes in the appearance of blueberries.

2.6. Statistical analysis

Using IBM SPSS Statistics (IBM, USA), a one-way analysis of variance (ANOVA) was performed on all data from this study. The significance of differences among experimental groups was analyzed using Tukey's test, with $p < 0.05$ as the significance level.

3. Results and discussion

3.1. Structure features of GDCRs

3.1.1. FTIR spectra and XRD patterns

To explore the interactions between the components in the composite films, the ATR spectra of the films were analyzed. As shown in **Fig. 1a**, both CMC and DCMC exhibit similar absorption peaks at 3480 and 2900 cm^{-1}. The peak at 3480 cm^{-1} corresponds to the hydroxyl groups (−OH) in cellulose, while the peak at 2900 cm^{-1} is attributed to the C−H stretching vibration in cellulose (Parida et al. 2014; Yan et al. 2023). Additionally, the absorption peaks at 1150 and 1034 cm^{-1} are attributed to the C−C and C−O stretching vibrations of CMC, respectively (Kačuráková et al. 2000). Notably, the FTIR spectrum of DCMC shows a new peak at 1740 cm^{-1}, which corresponds to the C=O stretching vibration of aldehyde groups (Fan et al. 2001; Kholiya et al. 2016). This indicates that sodium periodate selectively oxidized the hydroxyl groups on CMC to aldehyde groups, as illustrated in **Fig. 1c**. Furthermore, the aldehyde content in DCMC was determined to be 61.57%. For GF, the peaks at 1643 cm^{-1} and 1549 cm^{-1} correspond to amide I (C=O stretching vibration) and amide II (N-H bending), respectively (Ye et al. 2022). Compared to the GF film, no new peaks were observed in other gelatin-based composite films, likely due to the relatively low amounts of DCMC and catechin/rare earth ions added. In the spectra of GDCR and GD film samples, the C=O tensile vibration absorption peak of the aldehyde functional group completely disappears. Additionally, no distinct characteristic peaks were detected, as the peaks corresponding to Schiff bases overlapped with the amide I bands of gelatin (Jia et al. 2021). The shifts in peak positions indicate a chemical reaction between gelatin and DCMC, likely involving the formation of Schiff bases.

To further investigate the role of DCMC and catechin/rare-earth ions in the gelatin matrix, XRD analysis

was conducted to examine the changes in crystallinity of GDCR films with varying DCMC content. As shown in **Fig. 1b**, the GF film exhibited two peaks at 2θ values of 7.53° and 22.48°, corresponding to the crystalline structure of gelatin (Kanmani and Rhim 2014). The XRD patterns of GD and GCR films were similar to the GF film, but with slightly lower peak intensities. This decrease in intensity occurred because the intermolecular interactions between gelatin and DCMC or catechins may significantly impact the rearrangement of gelatin molecules. After incorporating catechin/rare-earth ions into the gelatin/DCMC matrix, the overall intensity of the diffraction peaks of the GDCR films was further reduced. This reduction indicates that the added catechin/rare earth ions are well dispersed in the gelatin matrix, potentially due to the formation of amorphous cross-linking between DCMC, catechin/rare ions, and gelatin.

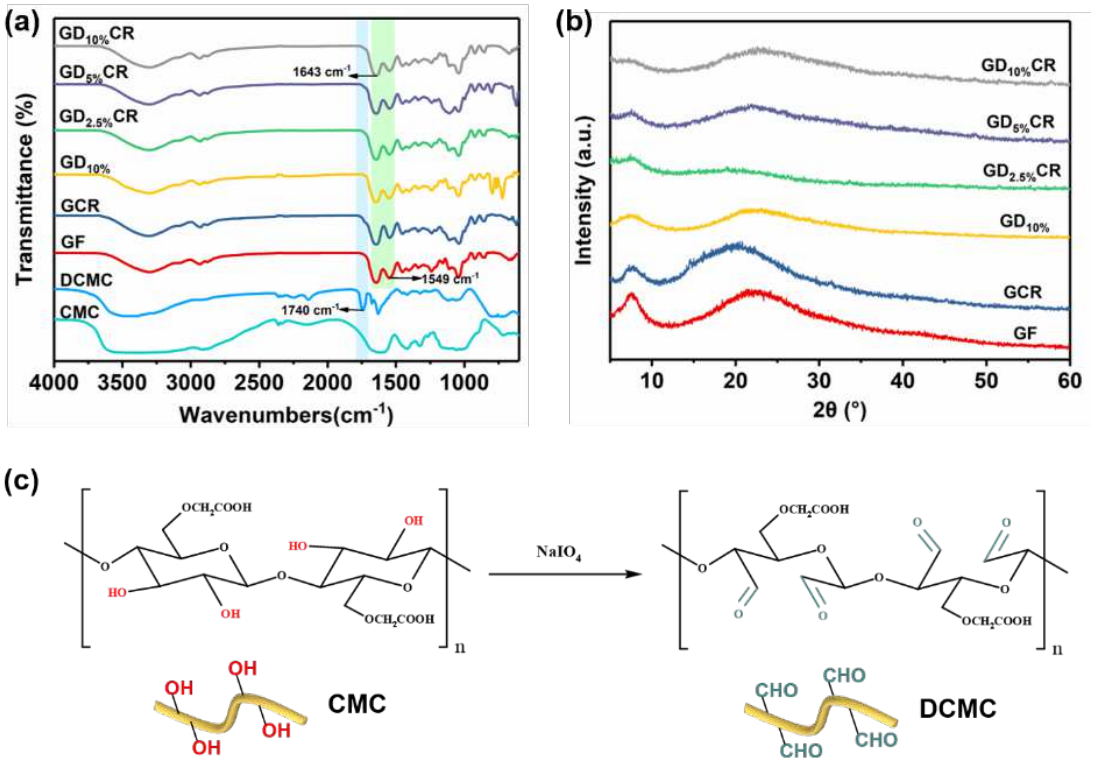
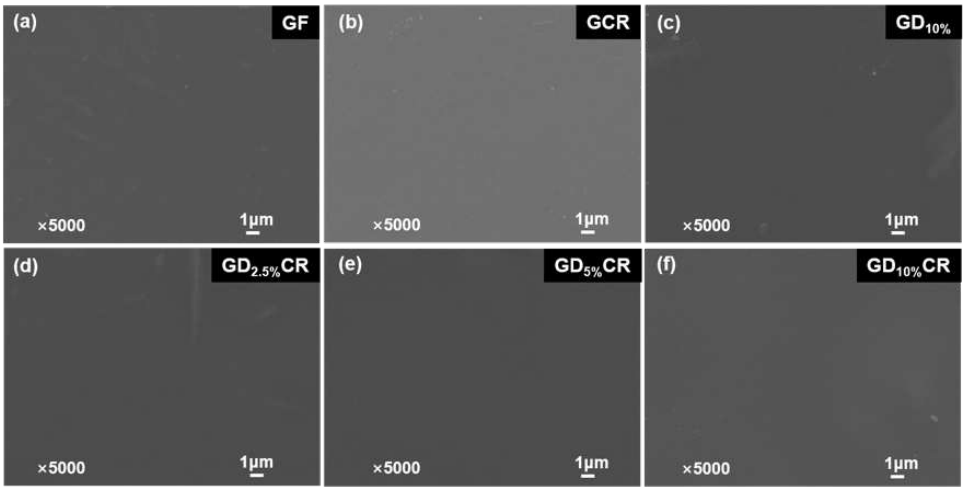


Fig. 1. ATR-FTIR spectra (**a**) and XRD patterns (**b**) of gelatin-based composite films; schematic diagram of DCMC synthesis (**c**).

306 *3.1.2. Microstructure of the composite films*

307 SEM was employed to observe the surface microstructure of the films. As demonstrated in **Fig. 2**, the
308 surface of the GF film is uniformly smooth, with no cracks or visible pores. After the addition of DCMC
309 or catechin/rare earth ions, slight wrinkles appeared on the surface of the $GD_{10\%}$ and GCR films. These
310 wrinkles were likely the result of intermolecular cross-linking between gelatin and DCMC or catechin
311 (Huang et al. 2023). However, the films remained smooth and uniform, indicating that the film components
312 were well compatible and that there was no phase separation. Additionally, the GDCR film exhibited a
313 uniformly smooth surface, and its structure remained relatively uniform and dense. This smoothness and
314 structural uniformity may be attributed to the excellent compatibility between the components and the
315 increased intermolecular interactions formed between the catechin, gelatin and DCMC.

316 

317 **Fig. 2.** SEM image of GF (**a**), GCR (**b**), $GD_{10\%}$ (**c**), $GD_{2.5\%}CR$ (**d**), $GD_{5\%}CR$ (**e**), and $GD_{10\%}CR$ (**f**).

318

319 **3.2. Physicochemical properties of the composite films**

320 *3.2.1. Optical properties*

321 The appearance color of the food packaging film is a key factor in its direct impact on consumer choice

and product acceptance. **Table 1** displays the color parameters, total color difference values, and transmittance at 280 nm and 660 nm for different films. Compared to the GF film, the direct incorporation of DCMC or catechin/rare earth ions into the GF film resulted in minimal changes to the L^*, a^*, b^*, and ΔE values, indicating that the introduction of DCMC or catechin/rare earth ions had a negligible impact on the overall color characteristics of the films ($GD_{10\%}$ and GCR films). However, when catechin/rare earth ions were introduced into the DCMC/gelatin-based films (i.e., GDCR films), significant changes in the L^*, a^*, b^*, and ΔE values were observed. This phenomenon suggests that catechin reacted with DCMC, potentially forming colored products (Sousa et al. 2005; Glavnik et al. 2009).

Table 1. Color parameters, total color difference, and transmittance of different films.

Films	L^*	a^*	b^*	ΔE	T_{280} (%)	T_{660} (%)
GF	73.9±0.1^{b}	-0.5±0.5^{d}	4.1±0.1^{e}	23.1±0.1^{e}	3.4±0.2^{a}	54.8±1.4^{a}
GCR	67.2±0.2^{c}	0.6±0.2^{c}	9.8±0.5^{c}	30.8±0.3^{d}	0.5±0^{c}	28.6±0.1^{c}
$GD_{10\%}$	75.1±0.1^{a}	-1.1±0.3^{d}	6.9±0.6^{d}	22.5±0.1^{f}	0.6±0.04^{b}	32.8±0.3^{b}
$GD_{2.5\%}$CR	40.2±1.0^{d}	16.8±0.3^{b}	36.3±0.3^{b}	68.9±0.8^{c}	0.3±0.01^{d}	26.7±0.3^{d}
$GD_{5\%}$CR	39.9±0.2^{d}	17.4±0.7^{ab}	40.1±0.5^{a}	71.4±0.6^{b}	0.3±0.01^{d}	22.3±1.0^{e}
$GD_{10\%}$CR	37.6±0.5^{e}	17.9±0.2^{a}	41.2±0.7^{a}	73.9±0.4^{a}	0.3±0.02^{d}	13.8±0.1^{f}

Different letters in the column indicated significant differences ($p < 0.05$).

As illustrated in **Fig. 3**, an aldehyde group in DCMC can be protonated to form a carbocation. This carbocation subsequently undergoes nucleophilic attack by 2 catechin molecules at C–6 or C–8 positions (Oliver et al. 2016). The L^* value, which reflects film brightness, gradually decreased as the DCMC content increased. Concurrently, the a^* and b^* values of the GDCR films increased as the DCMC content rose, likely due to a proportional relationship between product color intensity and DCMC content. Due to the

adverse effects of ultraviolet (UV) radiation, which can degrade food quality, it is essential to develop food packaging films with UV-blocking properties. The transmittance of various films can be observed in **Table 1**. The GF film exhibits a certain degree of transparency to both UV and visible light, with T_{280} and T_{660} values of 3.4% and 54.8%, respectively. The addition of DCMC significantly reduced both T_{280} and T_{660}, probably because of the formation of a structure between the DCMC and gelatin molecules. Furthermore, incorporating catechin and rare-earth ions contributed to a considerable decrease in T_{280} and T_{660}, likely due to the UV-absorbing properties of catechin, a polyphenolic compound. Notably, the GDCR films demonstrated nearly complete UV-blocking capabilities. The addition of both DCMC and catechin/rare earth ions resulted in significant reductions in UV transmission, while the transmittance of visible light decreased as the DCMC content increased. This behavior is likely due to the formation of a denser cross-linked structure among DCMC, catechin, and gelatin molecules, with cross-linking density increasing with the amount of DCMC added. These observations suggest that GDCR films can both offer effective UV protection and meet consumer expectations regarding the visual appeal of food packaging.

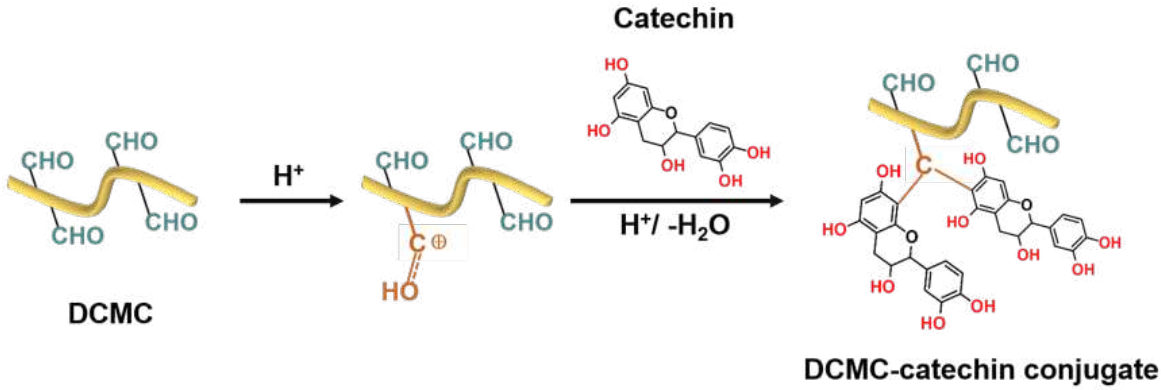
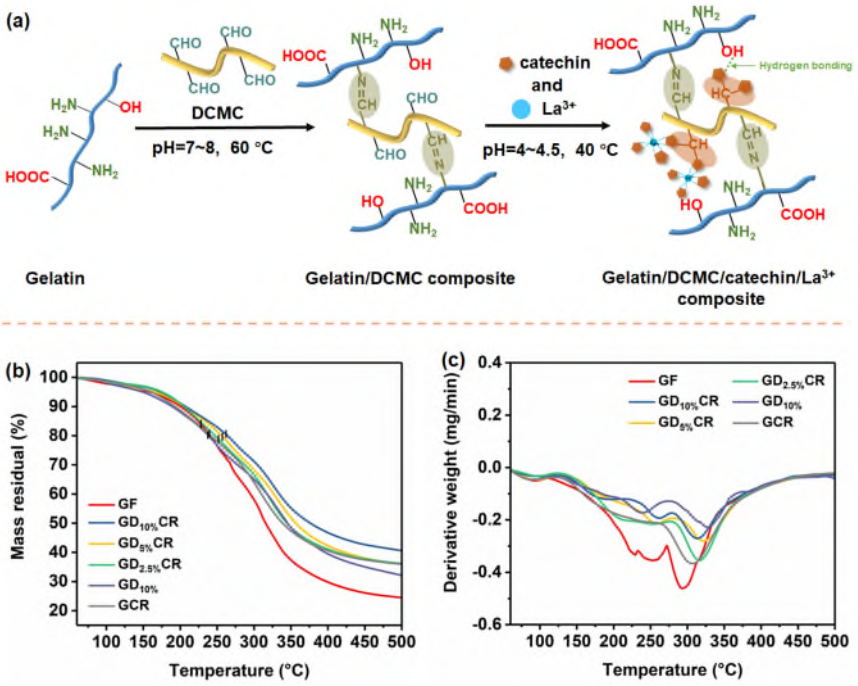


Fig. 3. Schematic diagram for the synthesis of DCMC-catechin conjugate through acid catalyzed condensation reaction.

3.2.2. Thermal stability

The thermal stability of gelatin is a crucial factor in the practical application of packaging films, as gelatin-based films tend to lose their integrity at high temperatures. To evaluate the thermal stability of the composite films, TGA and DTG were conducted. As shown in **Fig. 4b**, the amounts of DCMC and catechin/rare earth ions were relatively low during the preparation of the composite films, which resulted in similar TGA curves for the gelatin-based composite films. The DTG curves (as shown in **Fig. 4c**) reveal two weight loss stages. Notable rapid mass losses occurred at 228, 239, 238, 251, 257, and 262 °C for the GF, GCR, $GD_{10\%}$, $GD_{2.5\%}CR$, $GD_{5\%}CR$, and $GD_{10\%}CR$ films, respectively. The $GD_{10\%}CR$ film exhibited the highest thermal stability, followed by the $GD_{5\%}CR$ film, whereas the GF film demonstrated the lowest thermal stability. This improvement in thermal stability may result from covalent reactions between the amino groups of gelatin and the aldehyde groups of DCMC. Additionally, there were the potential reactions during the preparation of the films between the ortho- or para-active site of the catechin phenolic hydroxyl groups and the aldehyde groups of DCMC under acidic conditions, similar to what some researchers reported (Nonier et al. 2007, 2016; Hu et al. 2021; Yong et al. 2022). These covalent reactions led to a denser chemical cross-linking network in the GDCR film matrix (as shown in Fig. **4a**). In addition to covalent bonding, hydrogen bonding between catechin and gelatin may also contribute to the enhanced thermal performance of the GDCR films.



373

374 **Fig. 4.** Illustration of the reactions among gelatin, DCMC, and catechin/rare earth ions (**a**); TG (**b**) and DTG (**c**)

375 curves of the composite films.

376

377 *3.2.3. Mechanical properties*

378 Favorable mechanical properties of films are crucial for ensuring durability during food storage and

379 transportation, thereby reducing the likelihood of packaging damage and contamination. As shown in **Fig.**

380 **5**, the GF film exhibited the lowest tensile strength (TS) value of 22.39 MPa and an elongation at break (EB)

381 value of 3.74%. However, the incorporation of DCMC significantly improved both TS (29.75 MPa) and

382 EB (13.98%) of the $GD_{10\%}$ film, attributed to the formation of hydrogen bonding among the hydroxyl

383 groups of DCMC and the gelatin molecules, and the aldehyde group in the DCMC molecule reacts with

384 the amino group in the gelatin molecule, thereby forming a Schiff base structure. In general, films with

385 higher tensile strength may have lower elongation at break, as high-strength materials are often brittle and

386 more likely to fracture under tension. Although the high ductility material has low tensile strength, it can

remain intact under large deformation (Oyeoka et al. 2021; He et al. 2021; Thongsrikhem et al. 2022). To improve overall mechanical properties, the balance between TS and EB can be optimized by adjusting the formulation (Ke et al. 2023). When catechin/rare earth ions were incorporated into the DCMC/gelatin matrix to form GDCR films, their TS gradually increased, while the EB progressively decreased. Among the GDCR films, the TS value of $GD_{2.5\%}CR$, $GD_{5\%}CR$, and GD10%CR was 39.08 MPa, 45.27 MPa, and 46.37 MPa, respectively. Therefore, the $GD_{10\%}CR$ film demonstrated the highest TS, which was 23.98 MPa more than that of GF, and its TS was increased by 107.10%. Similarly, the TS of $GD_{2.5\%}CR$ and $GD_{5\%}CR$ was improved by 74.54% and 102.19%, respectively. This phenomenon is attributed to the covalent reactions between the amino groups of gelatin and the ortho- and para-active sites of the phenolic hydroxyl groups of catechin with the aldehyde groups of DCMC, resulting in a denser chemical cross-linking network in the GDCR film matrix. Moreover, hydrogen bonding may also occur between catechin and gelatin, providing additional enhancement of the mechanical performance of the GDCR films, consistent with the SEM and TGA analyses.

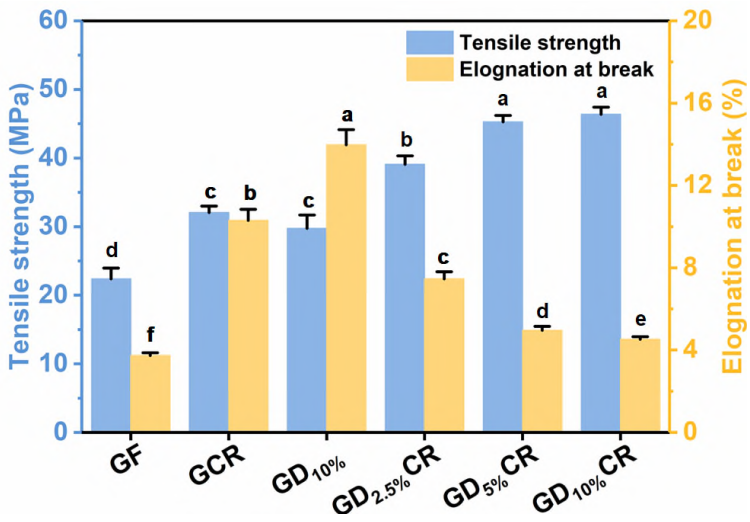


Fig. 5. TS and EB of the composite films.

3.2.4. Moisture and gas barrier performance

Effective moisture and gases barrier properties are crucial for food packaging, as they help reduce water vapor and gases (e.g, O_2 and CO_2) exchange between the food and its surrounding environment, thereby enhancing packaging conditions. As shown in **Fig. 6a**, the water vapor permeability (WVP) of the different films was evaluated. The GF film exhibited the highest WVP at 6.18×10^{-12} g/m·s·Pa, indicating the poorest water vapor barrier performance. After incorporating DCMC or catechin/rare earth ions into the gelatin-based films, the WVP significantly decreased compared to the GF film. The reduction in WVP of the $GD_{10\%}$ film can be caused by the cross-linking network formed by gelatin and DCMC through Schiff base interactions. For GCR membrane materials, the reduction in water-soluble protein content is mainly attributed to the hydrogen bond interaction formed between phenolic hydroxyl groups and gelatin molecules , which helps partially obstruct the water vapor transmission. Moreover, as the amount of DCMC added increased, the WVP of the GDCR films gradually decreased, with the $GD_{10\%}$CR film exhibiting the lowest WVP of 4.01×10^{-12} g/m·s·Pa. Besides, Figs. 6(b,c) show the O_2 permeability and CO_2 permeability performances of the composite films. The oxygen permeability coefficient (OPC) and carbon dioxide permeability coefficient (CPC) of the prepared composite film were significantly lower than the corresponding values of the GF film. Moreover, the GDCR films had much lower OPC and CPC than the GF, GCR, and GD films, and the OPC and CPC of GDCR films gradually decreased as the DCMC dosage increased, indicating better gas barrier performance.

The excellent moisture-proofing and gas-permeation resistance demonstrated by this material are attributed to the successful formation of its internal dense cross-linked network. This enhanced network structure arose from the synergistic integration of hydrogen-bonding interactions (from catechin),

coordination effects (from La^{3+}), and covalent Schiff base linkages (from DCMC), collectively reducing the free volume within the film matrix. Hydrogen bonding and coordination interactions among catechin, La^{3+}, and gelatin further enhanced the water-vapor and gas-barrier properties. Notably, potential reactions between the ortho- or para-active sites of the catechin phenolic hydroxyl groups and the aldehyde groups of DCMC contributed to the formation of a robust chemical cross-linking network within the GDCR film matrix, which likely improved gas barrier performance, highlighting its potential as an effective material for food packaging applications.

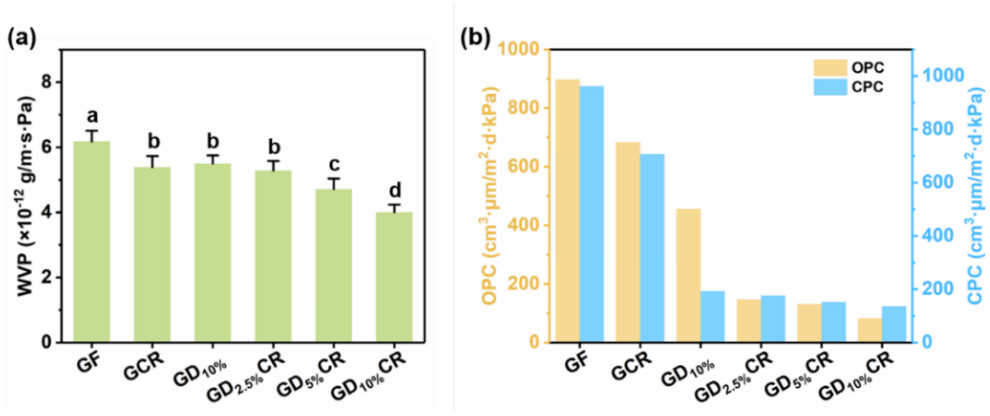


Fig. 6. Water vapor permeability (WVP) (**a**), and O_2 permeability coefficient (OPC) and CO_2 permeability coefficient (CPC) (**b**) of the composite films.

3.2.5 Sensitivity to water

Natural biopolymer materials, such as gelatin, are often inherently hydrophilic, which can pose significant challenges for their use in food packaging applications. To assess the hydrophilicity of various films, WCA, SB, and WS were evaluated for all film samples. As indicated in **Fig. 7**, both the GF and $GD_{10\%}$ films, which are rich in hydrophilic groups such as hydroxyl and carboxyl, exhibit poor water resistance, resulting in higher swelling ratios (W_{sb} = 32.12 and 28.88, respectively) and water solubilities (W_{ws} = 37.42% and

34.83%, respectively). The WCA values for these films were 105.79° and 102.82°, respectively, indicating high hydrophilicity. These hydrophilic interactions promote hydrogen bonding with water, which in turn reduces their resistance to water. In contrast, the GCR film exhibited significantly better water resistance, with a WCA of 111.53° and a W_{sb} of 14.02. This improvement can be attributed to the inherent hydrophobicity of catechin introduced into the gelatin matrix (Lin et al. 2018). On the other hand, during the preparation of the composite films, the hydroxyl groups on gelatin initially formed hydrogen bonds with the phenolic hydroxyl groups of catechin, thereby reducing the number of hydrogen bonds available for water interaction. As a result, the GDCR films demonstrated enhanced water resistance, lower swelling ratios, and reduced water solubility. The $GD_{10\%}CR$ film displayed the highest water resistance with a WCA of 113.93°, the lowest swelling ratio (W_{sb} = 4.39), and a water solubility of just 16.36%. These improvements were primarily due to covalent cross-linking between the amino groups of gelatin, the ortho- and para-active sites of the phenolic hydroxyl groups of catechin, and the aldehyde groups of DCMC, which enhanced the chemical cross-linking density within the films. In contrast, the GCR films formed through physical cross-linking *via* hydrogen bonding had higher water solubility, further highlighting the role of covalent bonding in improving the water resistance of the GDCR films.

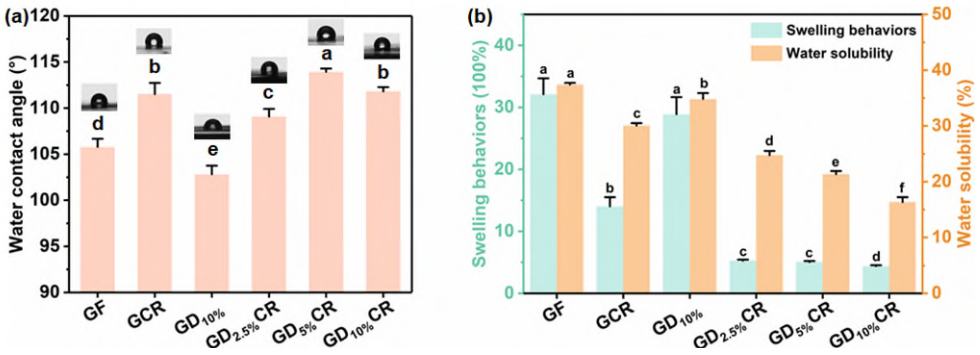
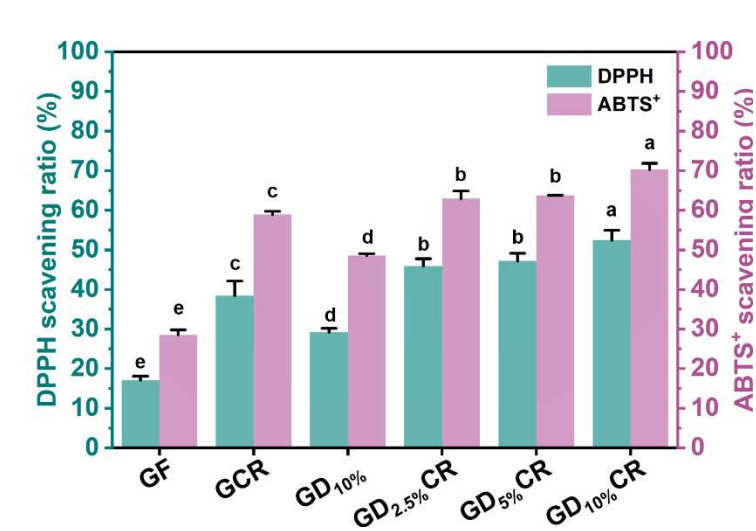


Fig. 7. Water contact angles (**a**) and swelling behavior and water solution (**b**) of the composite films.

3.3. Bioactivities

3.3.1. Antioxidant properties

Antioxidant capacity is an important property of food packaging materials, as it can slow food oxidation, reduce odor and color changes, help preserve vitamins and other nutrients, and extend shelf life. To evaluate the antioxidant capacity of the films, the DPPH and $ABTS^+$ radical-scavenging ratios of the film samples were determined. As shown in **Fig. 8**, the DPPH and $ABTS^+$ radical-scavenging ratios of different films exhibit a similar trend. The GF film showed the lowest scavenging ratio for both radicals (17.09% for DPPH and 28.55% for $ABTS^+$), indicating minimal antioxidant activity. This restricted activity arises from the presence of free amino and hydroxyl groups in gelatin, which can serve as proton or electron donors. The addition of DCMC markedly increased the free-radical scavenging rate of the GD10% membrane, likely due to the antioxidant properties of the Schiff base formed during the reaction. Moreover, the GCR film exhibited a higher radical-scavenging ratio than the GF and GD10% films, primarily owing to the strong antioxidant properties of catechin, a polyphenolic compound known for its high radical-scavenging ability. In the GDCR films, the combined effect of DCMC and catechin resulted in a significant increase in radical-scavenging ability ($p < 0.05$). The antioxidant activity was directly proportional to the DCMC content. The $GD_{10\%}CR$ film demonstrated the highest DPPH and $ABTS^+$ radical scavenging ratios, at 52.42% and 70.30%, respectively. Additionally, it is noteworthy that all film samples exhibited superior antioxidant activity against $ABTS^+$ radicals compared to DPPH radicals, possibly due to differences in the reaction systems: $ABTS^+$ radicals are aqueous, while DPPH radicals are alcohol-based, which affects their reactivity. These findings indicate that gelatin-based films incorporating DCMC and catechin/rare-earth ions exhibit significant antioxidant activity, making them highly suitable for active food packaging.



480

481 **Fig. 8.** DPPH and ABTS^{+} radical scavenging ratio of the composite films.

482

483 *3.3.2. Antibacterial properties*

484 The antibacterial efficacy of food packaging materials is crucial for effectively inhibiting microbial growth
485 and minimizing the likelihood of food deterioration. To assess the antibacterial performance of the films,
486 inhibition ratio tests were conducted against two common food spoilage pathogens: *E. coli* and *S. aureus*.
487 As shown in **Fig. 9**, the antibacterial activity of the GF film is the lowest because it serves as a nutrient
488 source for bacteria and creates an environment that promotes microorganism growth. In contrast, the GD10%
489 film exhibited minimal antibacterial activity against both bacterial strains, a phenomenon attributed to the
490 antimicrobial properties of the Schiff bases formed between DCMC and gelatin, which have previously
491 been associated with antibacterial effects (Yousif et al. 2017; Kaczmarek et al. 2018; Cui et al. 2023). The
492 GCR film also exhibited some antibacterial activity, likely due to catechin, a polyphenolic compound
493 known for damaging bacterial cell membranes. Catechin-induced damage increases film permeability and
494 osmosis, ultimately leading to bacterial cell death (Coppo and Marchese 2014; Nassarawa et al. 2023).
495 Furthermore, the incorporation of rare-earth ions into the films introduces active coordination properties

that can form catechin-rare-earth-ion complexes. These complexes exhibit additional antibacterial effects, potentially enhancing the overall antimicrobial activity of the composite films.

Compared with $GD_{10\%}$ film, the addition of catechin/rare-earth ions to DCMC/gelatin-based films significantly enhanced their antibacterial performance. This enhancement was more pronounced with increasing amounts of DCMC, which likely contributed to the formation of the catechin-rare earth ions complexes, producing a synergistic antibacterial effect. Experimental results showed that the $GD_{10\%}$CR film achieved inhibition ratios of 91.85% against *S. aureus* and 90.00% against *E. coli*, demonstrating the best antibacterial capability among the tested films. It is noteworthy that the antibacterial efficacy of all tested film samples against *S. aureus* was significantly greater than against *E. coli*. This difference may be attributed to structural differences in bacterial cell membranes, with S. aureus possessing a more susceptible membrane (Mostafa et al. 2023). Overall, the antibacterial performance test results show that $GD_{10\%}$CR film exhibits excellent antibacterial activity against both *E. coli* and *S. aureus*. This characteristic highlights its broad application prospects in food packaging.

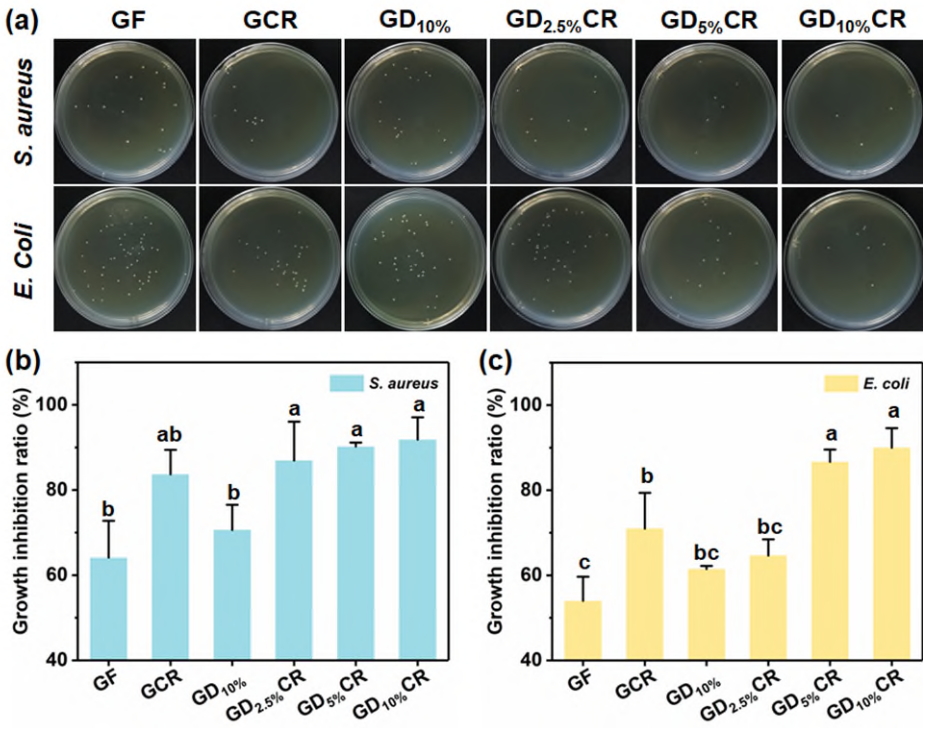


Fig. 9. Effect of the composite films on the growth of *E. coli* and *S. aureus* (**a**). Growth inhibition ratio of the films against *E. coli* (**b**) and *S. aureus* (**c**). Means within the same histogram followed by a different letter are significantly different ($p < 0.05$).

3.4. Packaging application for blueberries

The prepared composite film possesses excellent mechanical properties, outstanding antioxidant activity, and significant antibacterial ability. This comprehensive characteristic makes it highly applicable in the field of food packaging. To assess the practical feasibility of the prepared composite film as a food packaging material, this study used blueberries as the test material to conduct a preservation experiment. The investigation systematically examined the film's effectiveness in fruit packaging. Blueberries are perishable fruits and have a relatively short shelf life under natural conditions. Photographs of the spoilage process in blueberries packaged with composite films, stored for 4 days at room temperature, are shown in **Fig. 10**.

On the second day of the preservation experiment, the blueberries packaged in GDCR film exhibited vibrant color, maintained their shape, and displayed no indications of spoilage or fruit collapse. Concurrently, the blueberries packaged with alternative films began to deteriorate in texture, becoming noticeably soft and exhibiting slight white mold. On the fourth day of the preservation experiment, the blueberries packaged with the GDCR film displayed no signs of decay, maintaining good appearance, color, and plumpness. In contrast, those packaged with other films were nearly completely rotten, with substantial white mold growth present. Therefore, the GDCR composite film effectively enhanced the freshness preservation and substantially extended the shelf life of blueberries. The notable enhancement in fruit longevity is primarily attributable to the low WVP and the packaging material's superior antibacterial properties. The film's reduced WVP effectively retains moisture, minimizing loss and preserving the freshness of blueberries. Most importantly, the GDCR composite film exhibits favorable antibacterial properties, effectively inhibiting the growth and reproductive activity of microorganisms.

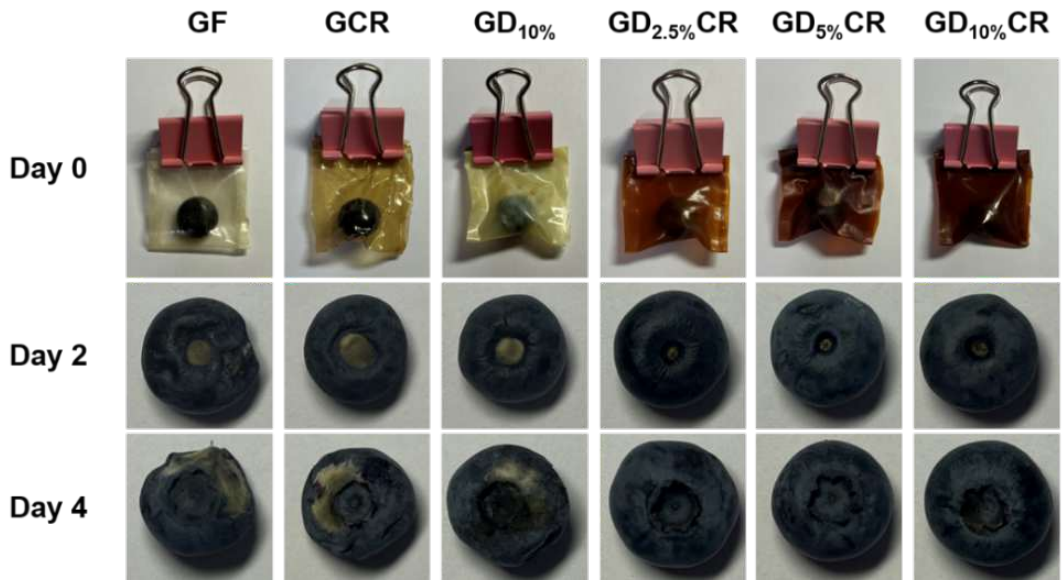


Fig. 10. Photographs of the spoilage process of blueberries packaged with the composite films stored at room temperature.

4. Conclusions

In this work, DCMC was successfully synthesized by the selective oxidation of CMC with sodium periodate. Subsequently, GDCR films with varying DCMC contents were successfully fabricated by incorporating DCMC and catechin/rare-earth ions. Compared with gelatin-based composite films without DCMC or catechin/rare-earth ions, the GDCR films exhibited enhanced thermal stability, mechanical strength, and UV-blocking properties. Additionally, these films exhibited reduced water vapor permeability, swelling ratio, and water solubility, which are critical factors for effective food packaging. These improvements can be attributed to the excellent compatibility and strong interactions among DCMC, catechin/rare earth ions, and gelatin. The reinforcing effects of DCMC and catechin/rare earth ions are primarily due to the covalent reactions between the amino groups of gelatin and the aldehyde groups of DCMC. Besides, there were potential reactions between the ortho- or para-active sites of the phenolic hydroxyl groups of catechin and the aldehyde groups of DCMC. Additionally, the possible hydrogen bonding between catechin and gelatin further enhances the crosslinking intensity of the GDCR films. These reactions contribute to a denser multipoint crosslinking network in the GDCR film matrix. Moreover, the incorporation of DCMC and catechin/rare earth ions significantly enhanced the antioxidant and antibacterial activities of the gelatin-based composite films. By integrating the aforementioned features, the GDCR composite films were used as packaging for blueberries, thereby enhancing preservation and significantly extending the fruit's shelf life. Overall, the optimized GDCR films exhibit the best comprehensive performance, showing significant advantages in both antibacterial properties and practical applications as packaging materials, demonstrating broad application potential in active food packaging.

Author Contributions

Wei Ding: Conceptualization, Methodology, Investigation, Writing – original draft, Funding acquisition. **Xuehai Gong:** Investigation, Writing – original draft. **Xinyue Wang:** Investigation. **Yanbei Wu:** Writing – review & editing, Resources, Funding acquisition. **Rong Wang:** Investigation. **Xi Qi:** Investigation. **Zhengyu Zhao:** Investigation. **Kanglei Wang:** Writing – review & editing, Visualization, Investigation, Data curation.

Competing interests

The authors declare no competing financial interest.

Data availability

The authors declare that the data supporting the results of this study are available within the paper. Data are available from the corresponding author upon reasonable request.

Acknowledgments

The authors were grateful for financial support from the Zhiyuan Science Foundation of Beijing Institute of Petrochemical Technology (2025001), the National Natural Science Foundation of China (22578009), and the Beijing Nova Program (Z211100002121085).

References

Al-Hassan AA, Norziah MH (2012) Starch–gelatin edible films: Water vapor permeability and mechanical

properties as affected by plasticizers. Food Hydrocoll 26:108–117. https://doi.org/10.1016/j.foodhyd.2011.04.015

Beghetto V, Conca S, Santandrea D (2026) Carboxymethyl Cellulose-Based Films for Sustainable Food Packaging: Modification Strategies and Structure–Property Relationships. Polymers 18:552. https://doi.org/10.3390/polym18050552

Białopiotrowicz T, Jańczuk B (2002) Surface Properties of Gelatin Films. Langmuir 18:9462–9468. https://doi.org/10.1021/la0201624

Caniça M, Manageiro V, Abriouel H, et al (2019) Antibiotic resistance in foodborne bacteria. Trends Food Sci Technol 84:41–44. https://doi.org/10.1016/j.tifs.2018.08.001

Cao N, Fu Y, He J (2007) Preparation and physical properties of soy protein isolate and gelatin composite films. Food Hydrocoll 21:1153–1162. https://doi.org/10.1016/j.foodhyd.2006.09.001

Carmen S (2021) Microbial capability for the degradation of chemical additives present in petroleum-based plastic products: A review on current status and perspectives. J Hazard Mater 402:123534. https://doi.org/10.1016/j.jhazmat.2020.123534

Coppo E, Marchese A (2014) Antibacterial Activity of Polyphenols. Curr Pharm Biotechnol 15:380–390. https://doi.org/10.2174/1389201015041408251211 42

Cui H, Cheng Q, Li C, et al (2023) Schiff base cross-linked dialdehyde β-cyclodextrin/gelatin-carrageenan active packaging film for the application of carvacrol on ready-to-eat foods. Food Hydrocoll 141:108744. https://doi.org/10.1016/j.foodhyd.2023.108744

Ding W, Guo S, Wang K, et al (2025) Aminated graphene oxide reinforced gelatin-chitosan composite films toward biopackaging: Preparation and properties. Int J Biol Macromol 284:138104.

https://doi.org/10.1016/j.ijbiomac.2024.138104

Ding W, Wang K, Liu H, et al (2024) Biomass-Derived Aldehyde and Aminated Graphene Oxide Reinforced Gelatin-Based Composite Films for Biopackaging via a Multipoint Cross-Linking Strategy. ACS Sustain Chem Eng 12:10624–10633. https://doi.org/10.1021/acssuschemeng.4c03622

Fakhouri FM, Costa D, Yamashita F, et al (2013) Comparative study of processing methods for starch/gelatin films. Carbohydr Polym 95:681–689. https://doi.org/10.1016/j.carbpol.2013.03.027

Fan QG, Lewis DM, Tapley KN (2001) Characterization of cellulose aldehyde using Fourier transform infrared spectroscopy. J Appl Polym Sci 82:1195–1202. https://doi.org/10.1002/app.1953

Fraga AN, Williams RJJ (1985) Thermal properties of gelatin films. Polymer 26:113–118. https://doi.org/10.1016/0032-3861(85)90066-7

Glavnik V, Simonovska B, Vovk I (2009) Densitometric determination of (+)-catechin and (−)-epicatechin by 4-dimethylaminocinnamaldehyde reagent. J Chromatogr A 1216:4485–4491. https://doi.org/10.1016/j.chroma.2009.03.026

He B, Wang Y, Jiang Z, et al (2021) Physical properties and antibacterial activity of the composited films based on carboxymethyl cellulose and gelatin functionalized with ε-polylysine. Int J Biol Macromol 191:1126–1136. https://doi.org/10.1016/j.ijbiomac.2021.09.181

Hu H, Yong H, Yao X, et al (2021) Highly efficient synthesis and characterization of starch aldehyde-catechin conjugate with potent antioxidant activity. Int J Biol Macromol 173:13–25. https://doi.org/10.1016/j.ijbiomac.2021.01.119

Huang H-L, Tsai I-L, Lin C, et al (2023) Intelligent films of marine polysaccharides and purple cauliflower

622 extract for food packaging and spoilage monitoring. Carbohydr Polym 299:120133.
623 https://doi.org/10.1016/j.carbpol.2022.120133
624 Jia F, Huang Y, Zhao J, et al (2021) Physicochemical and functional properties of dialdehyde
625 polysaccharides crosslinked gliadin film cooperated by citric acid. J Cereal Sci 102:103349.
626 https://doi.org/10.1016/j.jcs.2021.103349
627 Jiang X, Yang Z, Peng Y, et al (2016) Preparation, characterization and feasibility study of dialdehyde
628 carboxymethyl cellulose as a novel crosslinking reagent. Carbohydr Polym 137:632–641.
629 https://doi.org/10.1016/j.carbpol.2015.10.078
630 Kačuráková M, Capek P, Sasinková V, et al (2000) FT-IR study of plant cell wall model compounds: pectic
631 polysaccharides and hemicelluloses. Carbohydr Polym 43:195–203.
632 https://doi.org/10.1016/S0144-8617(00)00151-X
633 Kaczmarek MT, Zabiszak M, Nowak M, Jastrzab R (2018) Lanthanides: Schiff base complexes,
634 applications in cancer diagnosis, therapy, and antibacterial activity. Coord Chem Rev 370:42–54.
635 https://doi.org/10.1016/j.ccr.2018.05.012
636 Kamau-Devers K, Miller SA (2020) The environmental attributes of wood fiber composites with bio-based
637 or petroleum-based plastics. Int J Life Cycle Assess 25:1145–1159.
638 https://doi.org/10.1007/s11367-020-01744-6
639 Kanmani P, Rhim J-W (2014) Physicochemical properties of gelatin/silver nanoparticle antimicrobial
640 composite films. Food Chem 148:162–169. https://doi.org/10.1016/j.foodchem.2013.10.047
641 Karim AA, Bhat R (2008) Gelatin alternatives for the food industry: recent developments, challenges and
642 prospects. Trends Food Sci Technol 19:644–656. https://doi.org/10.1016/j.tifs.2008.08.001

643 Ke Q, Wang H, Huang X, et al (2023) Direct addition of vanillin improved the physicochemical properties
644 and antibacterial activities of gelatin/sodium carboxymethyl cellulose composite film. Ind Crops
645 Prod 206:117653. https://doi.org/10.1016/j.indcrop.2023.117653
646 Kholiya F, Chaudhary JP, Vadodariya N, Meena R (2016) Synthesis of bio-based aldehyde from seaweed
647 polysaccharide and its interaction with bovine serum albumin. Carbohydr Polym 150:278–285.
648 https://doi.org/10.1016/j.carbpol.2016.05.022
649 Kong P, Rosnan SM, Enomae T (2024) Carboxymethyl cellulose–chitosan edible films for food packaging:
650 A review of recent advances. Carbohydr Polym 346:122612.
651 https://doi.org/10.1016/j.carbpol.2024.122612
652 Kumari S, Rao A, Kaur M, Dhania G (2023) Petroleum-Based Plastics Versus Bio-Based Plastics: A
653 Review. Nat Environ Pollut Technol 22:1111–1124.
654 https://doi.org/10.46488/NEPT.2023.v22i03.003
655 Kurhade RR, Shaikh MS, Nagulwar V, Kale MA (2024) Advancements in carboxymethyl cellulose (CMC)
656 modifications and their diverse biomedical applications: a comprehensive review. Int J Polym
657 Mater Polym Biomater
658 Lee Y-E, Yoo S-H, Chung J-O, et al (2020) Hypoglycemic effect of soluble polysaccharide and catechins
659 from green tea on inhibiting intestinal transport of glucose. J Sci Food Agric 100:3979–3986.
660 https://doi.org/10.1002/jsfa.10442
661 Leopoldini M, Russo N, Toscano M (2011) The molecular basis of working mechanism of natural
662 polyphenolic antioxidants. Food Chem 125:288–306.
663 https://doi.org/10.1016/j.foodchem.2010.08.012

664 Lin Y-H, Tsai M-J, Fang Y-P, et al (2018) Microemulsion formulation design and evaluation for
665 hydrophobic compound: Catechin topical application. Colloids Surf B Biointerfaces 161:121–128.
666 https://doi.org/10.1016/j.colsurfb.2017.10.015
667 Liu J, Meng C, Yan Y, et al (2016) Structure, physical property and antioxidant activity of catechin grafted
668 *Tremella fuciformis* polysaccharide. Int J Biol Macromol 82:719–724.
669 https://doi.org/10.1016/j.ijbiomac.2015.11.027
670 Liu L, Xiao X, Li K, et al (2020a) Prevention of Bacterial Colonization Based on Self-Assembled Metal–
671 Phenolic Nanocoating from Rare-Earth Ions and Catechin. ACS Appl Mater Interfaces 12:22237–
672 22245. https://doi.org/10.1021/acsami.0c06459
673 Liu L, Xiao X, Li K, et al (2020b) Synthesis of Catechin-Rare Earth Complex with Efficient and Broad-
674 Spectrum Anti-Biofilm Activity. Chem Biodivers 17:e1900734.
675 https://doi.org/10.1002/cbdv.201900734
676 Lu Y, Luo Q, Chu Y, et al (2022) Application of Gelatin in Food Packaging: A Review. Polymers 14:436.
677 https://doi.org/10.3390/polym14030436
678 Luo Q, Hossen MA, Zeng Y, et al (2022) Gelatin-based composite films and their application in food
679 packaging: A review. J Food Eng 313:110762. https://doi.org/10.1016/j.jfoodeng.2021.110762
680 Luo Y, Wu Y, Wang Y, Yu L (Lucy) (2021) Active and Robust Composite Films Based on Gelatin and
681 Gallic Acid Integrated with Microfibrillated Cellulose. Foods 10:2831.
682 https://doi.org/10.3390/foods10112831
683 Mendoza-Wilson AM, Glossman-Mitnik D (2006) Theoretical study of the molecular properties and
684 chemical reactivity of (+)-catechin and (−)-epicatechin related to their antioxidant ability. J Mol

685 Struct THEOCHEM 761:97–106. https://doi.org/10.1016/j.theochem.2006.01.001
686 Mira L, Tereza Fernandez M, Santos M, et al (2002) Interactions of Flavonoids with Iron and Copper Ions:
687 A Mechanism for their Antioxidant Activity. Free Radic Res 36:1199–1208.
688 https://doi.org/10.1080/1071576021000016463
689 Mori R (2023) Replacing all petroleum-based chemical products with natural biomass-based chemical
690 products: a tutorial review. RSC Sustain 1:179–212. https://doi.org/10.1039/D2SU00014H
691 Mostafa H, Airouyuwaa JO, Hamed F, et al (2023) Structural, mechanical, antioxidant and antibacterial
692 properties of soy protein isolate (SPI)-based edible food packaging films as influenced by
693 nanocellulose (NC) and green extracted phenolic compounds from date palm leaves. Food Packag
694 Shelf Life 38:101124. https://doi.org/10.1016/j.fpsl.2023.101124
695 Nassarawa SS, Nayik GA, Gupta SD, et al (2023) Chemical aspects of polyphenol-protein interactions and
696 their antibacterial activity. Crit Rev Food Sci Nutr 63:9482–9505.
697 https://doi.org/10.1080/10408398.2022.2067830
698 Nazmi NN, Isa MIN, Sarbon NM (2017) Preparation and characterization of chicken skin gelatin/CMC
699 composite film as compared to bovine gelatin film. Food Biosci 19:149–155.
700 https://doi.org/10.1016/j.fbio.2017.07.002
701 Nonier M-F, Vivas N, Vivas de Gaulejac N, et al (2007) A kinetic study of the reactions of (+)-catechin
702 with aldehydes derived from toasted oak. J Sci Food Agric 87:2081–2091.
703 https://doi.org/10.1002/jsfa.2968
704 Oliver S, Thomas DS, Kavallaris M, et al (2016) Efficient functionalisation of dextran-aldehyde with
705 catechin: potential applications in the treatment of cancer. Polym Chem 7:2542–2552.

https://doi.org/10.1039/c6py00228e

Omerović N, Djisalov M, Živojević K, et al (2021) Antimicrobial nanoparticles and biodegradable polymer composites for active food packaging applications. Compr Rev Food Sci Food Saf 20:2428–2454. https://doi.org/10.1111/1541-4337.12727

Oyeoka HC, Ewulonu CM, Nwuzor IC, et al (2021) Packaging and degradability properties of polyvinyl alcohol/gelatin nanocomposite films filled water hyacinth cellulose nanocrystals. J Bioresour Bioprod 6:168–185. https://doi.org/10.1016/j.jobab.2021.02.009

Parida C, Dash SK, Pradhan C (2014) FTIR and Raman Studies of Cellulose Fibers of *Luffa cylindrica*. Open J Compos Mater 05:5. https://doi.org/10.4236/ojcm.2015.51002

Qiao C, Ma X, Zhang J, Yao J (2017) Molecular interactions in gelatin/chitosan composite films. Food Chem 235:45–50. https://doi.org/10.1016/j.foodchem.2017.05.045

Robinson L, Miller R (2015) The Impact of Bisphenol A and Phthalates on Allergy, Asthma, and Immune Function: a Review of Latest Findings. Curr Environ Health Rep 2:379–387. https://doi.org/10.1007/s40572-015-0066-8

Santandrea D, Beghetto V (2025) 4-(4,6-Dimethoxy-1,3,5-triazin-2-yl)-4-methyl-morpholinium chloride-assisted amide crosslinking of carboxymethyl cellulose for high-performing films. RSC Adv 15:34846–34860. https://doi.org/10.1039/D5RA05273D

Singh AP, Devi AS (2019) Bio-Plastics: A sustainable alternative to conventional petroleum based plastics. 4:

Sousa C, Mateus N, Perez-Alonso J, et al (2005) Preliminary Study of Oaklins, a New Class of Brick-Red Catechinpyrylium Pigments Resulting from the Reaction between Catechin and Wood Aldehydes.

J Agric Food Chem 53:9249–9256. https://doi.org/10.1021/jf051970e

Sun F, Shan P, Liu B, et al (2024) Gelatin-based multifunctional composite films integrated with dialdehyde carboxymethyl cellulose and coffee leaf extract for active food packaging. Int J Biol Macromol 263:130302. https://doi.org/10.1016/j.ijbiomac.2024.130302

Thongsrikhem N, Taokaew S, Sriariyanun M, Kirdponpattara S (2022) Antibacterial activity in gelatin-bacterial cellulose composite film by thermally crosslinking with cinnamaldehyde towards food packaging application. Food Packag Shelf Life 31:100766. https://doi.org/10.1016/j.fpsl.2021.100766

Threlfall EJ, Ward LR, Frost JA, Willshaw GA (2000) The emergence and spread of antibiotic resistance in food-borne bacteria. Int J Food Microbiol 62:1–5. https://doi.org/10.1016/S0168-1605(00)00351-2

Tyuftin AA, Kerry JP (2021) Gelatin films: Study review of barrier properties and implications for future studies employing biopolymer films. Food Packag Shelf Life 29:100688. https://doi.org/10.1016/j.fpsl.2021.100688

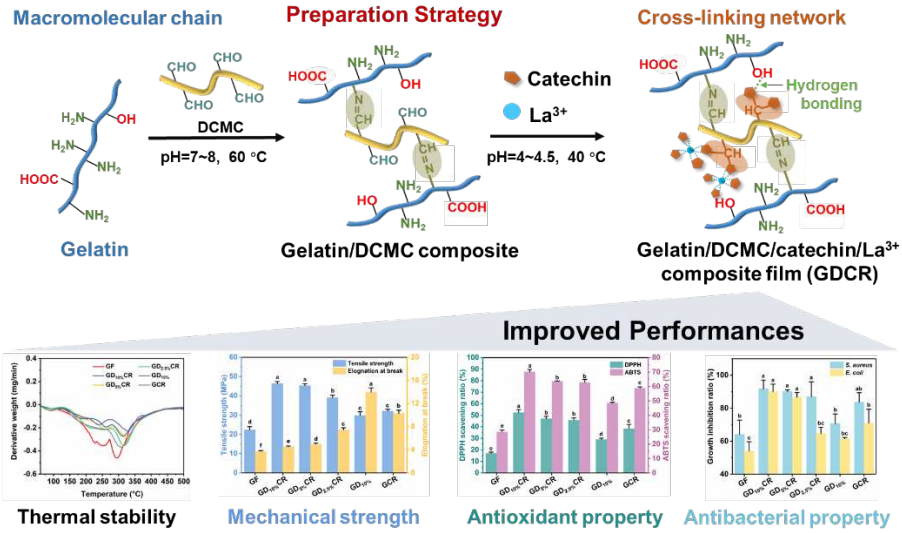
Wang P, He H, Cai R, et al (2019) Cross-linking of dialdehyde carboxymethyl cellulose with silk sericin to reinforce sericin film for potential biomedical application. Carbohydr Polym 212:403–411. https://doi.org/10.1016/j.carbpol.2019.02.069

Wu Y, Yu X, Ding W, et al (2023) Fabrication, performance, and potential environmental impacts of polysaccharide-based food packaging materials incorporated with phytochemicals: A review. Int J Biol Macromol 249:125922. https://doi.org/10.1016/j.ijbiomac.2023.125922

Yan L, Dang X, Yang M, et al (2023) Novel Hyperbranched Dialdehyde Carboxymethyl Cellulose-Grafted

748 Gelatin Films as Potential Natural Antibacterial Materials. ACS Sustain Chem Eng 11:7323–7333.
749 https://doi.org/10.1021/acssuschemeng.2c07302
750 Ye X, Liu R, Qi X, et al (2022) Preparation of bioactive gelatin film using semi-refined pectin reclaimed
751 from blueberry juice pomace: Creating an oxidation and light barrier for food packaging. Food
752 Hydrocoll 129:107673. https://doi.org/10.1016/j.foodhyd.2022.107673
753 Yin Y, Wai Woo M (2024) Transitioning of petroleum-based plastic food packaging to sustainable bio-
754 based alternatives. Sustain Food Technol 2:548–566. https://doi.org/10.1039/D4FB00028E
755 Yong H, Hu H, Wang Z, et al (2022) Structure, stability and antioxidant activity of dialdehyde starch grafted
756 with epicatechin, epicatechin gallate, epigallocatechin and epigallocatechin gallate. J Sci Food
757 Agric 102:6373–6386. https://doi.org/10.1002/jsfa.12003
758 Yousif E, Majeed A, Al-Sammarrae K, et al (2017) Metal complexes of Schiff base: Preparation,
759 characterization and antibacterial activity. Arab J Chem 10:S1639–S1644.
760 https://doi.org/10.1016/j.arabjc.2013.06.006
761 Yu X, Weng C, Zhang H, et al (2022) 'Multiple and short-range' cross-linking of dialdehyde carboxymethyl
762 cellulose contributes to regulating the physicochemical property of collagen fibril. Int J Biol
763 Macromol 219:21–30. https://doi.org/10.1016/j.ijbiomac.2022.07.142
764 Z. Naser A, Deiab I, M. Darras B (2021) Poly(lactic acid) (PLA) and polyhydroxyalkanoates (PHAs),
765 green alternatives to petroleum-based plastics: a review. RSC Adv 11:17151–17196.
766 https://doi.org/10.1039/D1RA02390J
767
768

Graphical Abstract



A novel, robust, and bioactive gelatin-based composite film was successfully fabricated by incorporating biomass-derived aldehydes, catechin, and rare earths.